2-phenylethynesulfonamide (PES) uncovers a necrotic process regulated by oxidative stress and p53

Paolo Mattiolo[a,1], Ares Barbero-Farran[a,1], Víctor J. Yuste[b], Jacint Boix[a,2] and Judit Ribas[a,2*]

[a] Pharmacology Unit, Departament de Medicina Experimental, Universitat de Lleida, IRBLLEIDA, Ed. Biomedicina 1, Av. Rovira Roure 80, 25198 Lleida, Catalunya, Spain

[b] Cell Death, Senescence, and Survival Group, Departament de Bioquímica i Biologia Molecular and Institut de Neurociències, Facultat de Medicina, Universitat Autònoma de Barcelona, Campus de Bellaterra, 08193 Barcelona, Catalunya, Spain

*To whom correspondence should be addressed:
Judit Ribas, Pharmacology Unit, DME, Ed. Biomedicina 1, Av. Rovira Roure 80, 25198 Lleida, Spain, Tel.: +34 973702404; E-mail: judit.ribas@mex.udl.cat

ABSTRACT

2-phenylethynesulfonamide (PES) or pifithrin-μ is a promising anticancer agent with preferential toxicity for cancer cells. The type of cell death and the molecular cascades activated by this compound are controversial. Here, we demonstrate PES elicits a caspase- and BAX/BAK-independent non-necroptotic necrotic cell death, since it is not inhibited by Necrostatin-1. This process is characterized by an early generation of reactive oxygen species (ROS) resulting in p53 up-regulation. Accordingly, thiolic antioxidants protect cells from PES-induced death. Furthermore, inhibiting the natural sources of glutathione with L-buthionine-sulfoximine (BSO) strongly cooperates with PES in triggering cytotoxicity. Genetically modified p53-null or p53 knocked-down cells show resistance to PES-driven necrosis. The predominant localization of p53 in chromatin-enriched fractions added to the up-regulation of the p53-responsive gene p21, strongly suggest the involvement of a transcription-dependent p53 program. On the other hand, we report an augmented production of ROS in p53-positive cells that, added to the increased p53 content in response to PES-elicited ROS, suggests that p53 and ROS are mutually regulated in response to PES. In sum, p53 up-regulation by ROS triggers a positive feedback loop responsible of further increasing ROS production and reinforcing PES-driven non-necroptotic necrosis.

Keywords

Anticancer drug; necrosis; p53; reactive oxygen species (ROS); 2-phenylethynesulfonamide (PES); pifithrin-μ

Chemical compounds

2-phenylethynesulfonamide (Pubmed CID 327653)

L-buthionine-sulfoximine (Pubmed CID 119565)

N-Acetyl Cysteine (Pubmed CID 12035)

Dithiothreitol (Pubmed CID 19001)

Necrostatin-1 (Pubmed CID 282833)

3-methyladenine (Pubmed CID 1673)

Q-VD-OPh (Pubmed CID 11237609)

1. Introduction

PES (2-phenylethynesulfonamide), also named pifithrin-μ, was first identified as a compound able to repress apoptosis induced by the translocation of p53 to the mitochondria [1]. Further studies have revealed that PES is an effective inducer of cell death with increased selectivity for cancer cells [2]. The pharmacological actions of PES include the blockage of both the proteasome and the autophagic process [3]. These to actions converge in increasing the proteotoxic stress of the highly metabolically-active cancer cells but, also, in inactivating proteins, such as p53, through its inclusion in insoluble aggregates [3]. This p53 inactivating mechanism, plus the fact that p53-defective cells are not resistant to PES, has supported the idea of a null involvement of p53 in the process of cell death triggered by this molecule. Cell death, cell cycle arrest, senescence, DNA repair, glucose metabolism, ROS generation and autophagy are some of the cellular phenomena regulated by p53 [4]. p53 is the most frequently mutated tumor suppressor gene in human cancer [5,6]. Most cellular insults trigger intracellular signaling cascades that converge in p53 activation, for example DNA damage, viral infection, oncogene activation or ROS generation [4,7]. In response to these stimuli, p53 is stabilized and engages a plethora of molecular pathways, including both transcriptional and non-transcriptional events [4,8].

Necrotic cell death was initially described as a passive mechanism of cell demise. For a while, necrosis became synonym of accidental death and was defined by its morphological traits [9]. However, further research uncovered necrosis as a regulated process in many instances [10,11]. Necroptosis is a type of regulated necrosis mediated by the activation of receptor-interacting protein kinase 1 (RIPK1) and RIPK3.

Necrostatin-1 is a RIPK1 inhibitory drug, which allows the inhibition and identification of necroptotic cell death [12].

We set out to gain a better understanding of how PES kills cancer cells. PES elicited a non-apoptotic, non-autophagic, non-necroptotic cell death in SH-SY5Y and HCT116 cells. Interestingly, PES triggered an early burst on ROS content, which was required for cytotoxicity. We observed a ROS-dependent increase in the p53 protein levels, mostly located at the chromatin-enriched fraction and followed by an increase on p21 content. p53 up-regulation boosted cell sensitivity to PES-mediated necrosis. In this sense, silencing p53 diminished the cytotoxic response to PES. In sum, our results indicate that ROS produced by PES trigger the up-regulation of p53, which, in turn, increases the production of ROS, resulting in a non-necroptotic form of necrosis.

2. Material and Methods

2.1 Cell culture and drug treatments

Colon adenocarcinoma HCT116 and HCT116 p53-/- cells were obtained from Dr. Vogelstein's laboratory [13]. The immortalized MEF *Bax-/-Bak-/-* and their WT counterparts were obtained from Dr. Korsmeyer's laboratory [14,15]. SH-SY5Y, HEK293, U87MG, HeLa and HL-60 cell lines were obtained from the American Type Culture Collection. SH-SY5Y, HEK293, U87MG, HeLa and MEFs were maintained in DMEM, HL-60 in RPMI and all the colon-derived cells in McCoy's media. All media were

supplied by Lonza (Rockland, ME, USA) and supplemented with 10% FCS (Gibco part of Invitrogen, Paisley, UK). Plasmocin™ (InvivoGen, San Diego, CA, USA) at 5 µg/ml final concentration was added as a prophylactic antibiotic. Cultures were regularly PCR-tested to confirm mycoplasma-free conditions. Cultures were maintained at 37ºC in water-saturated, 5% CO_2 atmosphere. Stock solutions of PES and the other chemicals were prepared in DMSO. From these stock solutions, drugs were delivered to the culture media and adjusted to the final concentrations reported in the text and figures. The serial dilution procedure was used in concentration-dependency determinations.

2.2 Chemical reagents

CellTiter 96® kit containing the reagent MTS (3-(4,5-dimethylthiazol-2-yl)-5-(3-carboxy-methoxy phenyl)-2-(4-sulfophenyl)-2H-tetrazolium) was provided by Promega (Madison, WI, USA). Pierce Biotechnology (Rockford, IL, USA) provided Alamar blue™ Cell Viability Assay Reagent. Q-VD-OPh (Q-Val-Asp(non-methylated)-OPh) and 3-methyladenine (3-MA) were obtained from Calbiochem part of Merck KGaA (Darmstadt, Germany). AcDEVDafc (Acetyl-Asp-Glu-Val-Asp-7-amino-4-trifluoromethyl-coumarin) was purchased from Enzo Life Sciences (Farmingdale, NY, USA). Dithiothreitol (DTT) was from Thermo Fisher Scientific (Waltham, MA, USA). Necrostatin-1 was purchased from Tocris Bioscience (Ellisville, MI, USA). Staurosporine (STS), Spautin-1, bisBenzimide (Hoechst 33342), PI (Propidium iodide), N-acetyl-L-cysteine (NAC) and L-buthionine-sulfoximine (BSO) were supplied by Sigma-Aldrich (St. Louis, MO, USA). Unless otherwise stated, the non-listed reagents were also from Sigma.

2.3 Cell survival and cell death and nuclear morphology assessment

To determine cell survival, MTS or Alamar blue reagents were used indistinctly. Both assays couple a nonspecific cellular reductase activity of viable cells to the reduction of a dye into colored (MTS) or fluorescent (Alamar blue) products, which are subsequently quantified. Percentage of viability was obtained by referring these values to the ones obtained with a population of vehicle treated cells. To assess cell death, cultures stained with PI, were trypsinized and subjected to flow cytometry analysis. Nuclear morphology was observed by direct fluorescence microscopy of cells in media containing 0.05 µg/ml bisBenzimide plus 12.5 µg/ml PI as previously described [11].

2.4 Caspase activity

Effector caspase activation (DEVDase activity) was obtained by quantifying the fluorescence released from Ac-DEVD-afc substrate after incubation at 37°C in the lysed cell cultures. This method has been validated and described in our previous work [16].

2.5 Overexpression of p53

HCT116 p53-/- cells, plated at 1.2 x 10^6 in p35 wells, were transfected with 6 µg of pCMV-Neo-Bam p53 WT or pCMV-Neo-Bam [17] in combination with 0.6 µg of a plasmid containing GFP. DNA was prepared in Opti-MEM^{TM} media (Life Technologies,

Carlsbad, CA, USA) before adding Turbofect transfection reagent (Thermo Fisher Scientific, Waltham, MA, USA) as described in the instructions manual. After 24 h, cells transfected were plated in M96 plates for drug treatment and cell viability assessment.

2.6 Lentiviral production and infection

FSV and FSV p53 lentiviral constructs were gently provided by Dr. Xavier Dolcet and Dr. Núria Eritja. Vectors contained a U6 promoter for expression of short hairpin RNAs against p53 (GTCCAGATGAAGCTCCCAGAA) and the Venus variant of YFP under the control of an SV40 promoter for monitoring transduction efficiency. Lentiviral particles were produced in 293T cells co-transfected by the calcium phosphate method with the above plasmid plus plasmids coding for the envelope and the packaging systems (VSV-G and Δ8.9, respectively). The day after transfection, 293T cells were switched to media containing no anti-mitotics and left for 2–3 days. Supernatants were then harvested, filtered through a 0.45 μm filter, and directly added to cultures in the presence of Polybrene (Merck Millipore part of Merck KGaA, Darmstadt, Germany).

2.7 Electron microscopy

Cells were collected, washed twice in PBS (150 mM ClNa, 2.7 mM ClK, 8 mM Na_2HPO_4, 1.5 mM KH_2PO_4) and fixed for 30 min at 4 °C in 100 mM phosphate buffer (pH 7.4) containing 2.5% glutaraldehyde. After rinsing the pellets twice with PBS at 4 °C, the cells were post-fixed in buffered OsO_4, dehydrated in graded acetone and

embedded in Durcupan® ACM resin (Sigma-Aldrich, St. Louis, MI, USA). Ultrathin sections mounted on copper grids were counterstained with uranyl acetate and lead citrate. A transmission electron microscope (Zeiss EM 910) was employed to visualize the cellular ultrastructure.

2.8 Intracellular ROS measurement

The quantification of intracellular ROS was based on fluorescence of the compound DCF that results from cell metabolization and ROS action on the precursor compound 2',7'dichlorofluorescin diacetate. Briefly, cells were seeded in 96 well plates. Media was replaced 48 h later by Phenol-red free Hank's Balanced Salt Solution containing 10 µM DCF. After an incubation of 30 min, the reagent was removed and cells were washed with pre-warmed PBS. Cultures were then immediately incubated in full media containing the investigated drug. At the times desired, fluorescence was read at 485/530 nm (excitation/emission wavelengths) with a plate reader (Infinite® M200, Tecan, Maennedorf, Switzerland).

2.9 Protein extraction and Western blotting

To perform whole cell extracts, cells were lysed in a buffer containing 100 mM Tris/ClH pH 6.8, 1% SDS, 1 µM EDTA, plus the cocktail of protease inhibitors from Sigma followed by sonication. After a centrifugation at 12,000 × *g* for 15 min, a total protein extract was obtained. To obtain extracts from specific cell subfractions

(cytosolic, nucleoplasmic and chromatin-enriched), we followed the protocol described in a previous publication [18]. The protein concentration was determined by means of the DC Protein Assay (BioRad, Hercules, CA, USA). Volumes were calculated to equalize the protein load in SDS 12%-polyacrylamide gel electrophoresis. Following electrotransfer to 0.45 µm PVDF membranes (EMD Millipore part of Merck KGaA, Darmstadt, Germany), we applied the following antibodies: anti-p53 clone BP53-12 (Upstate, part of Merck KGaA, Darmstadt, Germany), anti-p21 clone CP74 (Sigma, St. Louis, MI, USA), anti-lactate dehydrogenase (LDH) (Rockland™ Immunochemicals Inc., Boyertown, PA, USA), anti-polypyrimidine tract binding protein 1 (PTBP1) ab5642 (Abcam, Cambridge, England, UK) and anti-GAPDH-Peroxidase clone GAPDH-71.1 (Sigma, St. Louis, MI, USA). Immunoblots were finally developed with the Immobilon™ reagent from Millipore part of Merck KGaA (Darmstadt, Germany). Chemiluminiscence was recorded and densitometric analysis was performed by means of a Chemidoc™ apparatus and the Image Lab version 4.0.1 software from Bio-Rad. To quantify expression of p53, values of signal intensity were normalized to the appropriate signal in control extracts. Alternatively, to quantify p53 or p21 content in Fig. 6B or Fig. 7A, values of signal intensity were first referred to the values of GAPDH and then, normalized to a non-induced condition.

3. Results

3.1 PES triggers caspase-independent non-apoptotic cell death

A panel of human-derived cell lines (SH-SY5Y from neuroblastoma, U87MG from grade III astrocytoma, HL-60 from acute promyelocytic leukemia, HEK293 from embryonic kidney, HeLa from cervical cancer, and HCT116 from colorectal carcinoma) was used to assay the cytotoxicity induced by increasing concentrations of PES. As shown in Fig. 1A, PES triggered loss of cell viability in a concentration-dependent manner. In support of previous observations, the non-tumor derived HEK293 cells displayed a greater resistance to PES-driven toxicity [2]. We focused our research on HCT116 and SH-SY5Y, two tumor-derived cell lines with different ontogeny, being SH-SY5Y neatly more sensitive to PES than HCT116. Plasmatic membrane rupture by means of PI permeability was evaluated over time at concentrations of 12.5 and 25 μM PES in SH-SY5Y and HCT116, respectively. As shown in Figs. 1, B and C, 12.5 μM PES for 24 h in SH-SY5Y was equivalent to 25 μM for 48 h in HCT116. At these concentrations, 60% of SH-SY5Y and HCT116 cells were PI positive after 24 h and 48h, respectively. To assess whether the type of cell death was apoptotic, we double stained nuclei with bisBenzimide and Propidium iodide (PI). In these experiments, HCT116 and SH-SY5Y did not present evident chromatin condensation or nuclear fragmentation, which are distinctive traits of apoptosis. A similar behavior was observed in U87MG, HeLa, 293HEK and HL-60 cells when assaying concentrations of PES that at 24 h triggered death in 50% of the cell populations (results not shown). To sustain the absence of apoptotic death in HCT116 and SH-SY5Y, caspase activation (DEVDase activity) was evaluated through time. As expected, PES was unable to trigger caspase activation in both cell lines (Figs. 2A and B). As a control, we assessed caspase activity

in response to Staurosporine (STS), thus confirming the caspase functionality in both cell lines (Figs. 2A and B). Equivalent results were obtained when applying the same strategy to U87MG, HeLa, 293HEK and HL-60 cells (Fig. 2C). To further discard apoptosis as the predominant death process engaged by PES, we tested its effects on mouse embryonic fibroblasts (MEFs) defective in both, BAX and BAK. These proteins are key positive mediators at the mitochondrial or intrinsic pathway of apoptosis and, therefore, MEF *Bax-/-Bak-/-* cells become completely unresponsive to the stimuli that trigger it. As expected, MEF *Bax-/-Bak-/-* cells displayed resistance to STS as compared to their WT counterparts. However, deficiency of BAX and BAK provided no protection when cells were treated with PES (Fig. 2D). Altogether these results indicated that PES was triggering caspase- and BAX/BAK-independent cell death in HCT116 and SH-SY5Y cells and suggested the involvement of a necrotic type of cellular demise.

3.2 PES induces a non-necroptotic, necrotic type of cell death

Depending on the cellular model, PES either elicits caspase-independent [2,19] or caspase-dependent [20–22] cell death, or a mixture of both [23]. To gain insight on the kind of cell death induced by PES, we evaluated the protective effects of commonly used inhibitors of death. Blockage of either apoptosis with the broad caspase inhibitor Q-VD-OPh, necroptosis with RIPK1 inhibitor Necrostatin-1 or autophagy-driven cell death with 3-MA or Spautin-1, proved to be inefficient strategies to avoid PES-triggered cell death (Fig. 3A). Morphological studies by electronic microscopy remain one of the best methods to ascertain necrosis [9]. HCT116 cells displayed a morphological

phenotype consistent with its origin in colon epithelia, with cells establishing junctions at the contact sites and displaying mitochondria and Golgi apparatus in a polarized way at a side of the nucleus (Fig. 3B). Upon PES treatment, HCT116 cells underwent mitochondrial disruption and an increased cytoplasm vacuolization (Fig. 3C). Later in the process, cell membrane became ruptured and the cytoplasm severely unstructured (Fig. 3D). These traits were consistent with a necrotic type of cell death. Similar morphological changes were observed in PES-challenged SH-SY5Y cells, with images of severely disrupted mitochondria only after 12 h of treatment (Fig. 3F). Together, these results indicated PES triggered a non-necroptotic, necrotic type of cell death.

3.3 ROS are pivotal elements in necrosis driven by PES

When the intracellular antioxidant systems are overloaded, the excess of ROS leads to oxidative stress, to the damage of essential biological components and, eventually, to necrosis [9]. In an attempt to establish a potential link between PES-driven necrosis and oxidative stress, we monitored the induction of ROS by PES in a time-dependent manner. At merely 30 min of PES treatment, we detected a significant increase in ROS content (Fig. 4A). To evaluate the relevance of the observed ROS in PES-driven necrosis, we assessed the effects of thiolic antioxidants, such as dithiothreitol (DTT) and N-Acetyl Cysteine (NAC) and confirmed they conferred a significant protection to PES-mediated necrosis in both SH-SY5Y and HCT116 cells (Figs. 4B and C). Efficient suppression of ROS by either DTT or NAC in combination with PES was controlled and confirmed by ROS quantification (data not shown). These

findings were consistent with necrosis being a consequence of ROS build-up in response to PES. To further validate the central role of ROS in PES-induced necrosis, HCT116 and SH-SY5Y cells were challenged with combinations of PES and L-Buthionine sulphoximine (BSO). BSO is a specific inhibitor of γ-glutamylcysteine synthetase able to deplete the intracellular levels of glutathione [24,25]. BSO and the subsequent glutathione depletion are not toxic for most cells unless subjected to oxidative stress [26]. Therefore, HCT116 and SH-SY5Y cells were pre-incubated with BSO and exposed to sublethal concentrations of PES. Under these circumstances, we reported a significant increase of ROS content (Fig. 4D). Thus supporting BSO improves generation of ROS by PES. Next, we applied this combination to our experimental paradigms and assessed the impact on their survival. Accordingly, BSO strongly cooperated with sublethal concentrations of PES to trigger cell death in HCT116 and SH-SY5Y cells (Fig. 4E). This cooperation was also detected in other cell lines, for instance U87MG and HeLa cells, which were more resistant to PES-deadly actions (Fig. 1A). Together, these findings reinforced the involvement of ROS in PES-triggered necrosis.

3.4 p53 participates in PES-driven necrosis

p53 is a pivotal stress sensor that responds to a great variety of cell insults by orchestrating cell demise. Besides apoptosis and autophagic cell death, p53 is also involved in necrosis [27–29]. To ascertain the involvement of p53 in PES-triggered necrosis, we used HCT116 cells and their p53-deficient counterparts. HCT116 p53-/-

cells required higher concentrations of PES to get the same amount of cell death found in HCT116 cells, after 24 h of treatment (Fig. 5A). Indeed, leakage of the membrane in HCT116 p53-/- cells was significantly protected (15.6±8.1 % of PI-positive cells) when compared to HCT116 (45.5±7.7 % of PI-positive cells) (Fig. 5B). To better demonstrate the observed differences were due to p53 and not to unrelated phenomena, we reintroduced a functional p53 into HCT116 p53-/- cells. Transient transfection of p53 sensitized HCT116 p53-/- cells to PES-driven cell death (Fig. 5C). These data were in agreement with p53 being implicated in PES-driven necrosis.

3.5 p53 is predominantly located at the chromatin-enriched cellular fractions in response to PES

Since PES blocks the transcription-independent p53 translocation to mitochondria [1], we surmised the observed p53-dependent susceptibility could rely on its transcriptional activity, which consists in the regulation of a specific set of genes by binding to p53-responsive elements [30]. To do so, p53 needs to be located at the nucleus, more precisely at the chromatin-enriched fraction. Therefore, direct proof of this localization was necessary to substantiate p53 was modulating transcription of target genes. To experimentally find this evidence, we first interrogated the presence of p53 in chromatin-enriched fractions after challenging cells with PES. Using a previously described method to precisely separate cellular extracts into specific fractions [18], SH-SY5Y extracts were subfractionated into a cytoplasmic fraction, enriched in 0.1% triton-soluble proteins (C) and two nuclear fractions, one enriched in hydrosoluble proteins or

nucleoplasm (N1) and the other, containing the insoluble and chromatin-bound proteins (N2). In healthy non-treated SH-SY5Y cells, most of the p53 content was found in either nucleoplasmic- or chromatin-enriched fractions. However, after PES treatment, p53 was preferentially found in the chromatin-enriched fraction (Fig. 6A). Precisely, p53 surpassed the control by 3 folds in the nucleoplasmic fraction and 6 folds in the chromatinic one (Fig. 6A). Purity of the fractions was controlled by the presence of the cytoplasmic enzyme lactate dehydrogenase (LDH) and nuclear polypyrimidine tract binding protein 1 (PTBP1). These data supported that PES was up-regulating p53, which located at the nucleus, where probably it was triggering the transcription of p53-responsive genes involved in a form of oxidative stress-regulated necrotic cell death. To validate this up-regulation in a time-dependent manner, total levels of p53 in SH-SY5Y cells were studied over a 24 h period of treatment. A notable increase of p53 content was evident at 6 h, before any sign of necrosis occurred (aprox. 2.4 folds over time 0, Fig. 6B). In parallel, abundance of one of the best-known transcriptional targets of p53, p21 [31,32], was monitored. Kinetics of p21 paralleled those of p53 (Fig 6B). Similar results were obtained with HCT116 cells (not shown). Overall, these results were suggestive of a functional p53, activating transcription in response to PES. Finally, we considered that specific inhibition of p53 would be of paramount importance to assess its role in cell death. To do so, endogenous p53 was specifically silenced with a lentivirus carrying an shRNA against p53 (shp53). We observed an increase in the resistance of HCT116 (Fig. 6C) and SH-SY5Y (Fig. 6D) cells to PES-induced necrosis in any of the concentrations employed. Efficiency of p53 down-regulation was assessed

and found to be greater than 80% by Western-blot (data not shown). Therefore, we concluded that a p53-dependent program was involved in necrosis triggered by PES.

3.6 ROS and p53 form a positive feedback loop in PES-mediated necrosis

p53 can either be activated in response to oxidative stress or, alternatively, generate ROS through transcription-dependent mechanisms [7]. Several experiments were performed to distinguish between these two possibilities. First, SH-SY5Y cells were either treated with PES plus or minus DTT and p53 content was assessed by Western-blot (Fig. 7A). Cells challenged with PES up-regulated p53 by 35 folds compared with untreated cells. Although single DTT treatment increased p53 by 10 folds, combination of DTT and PES resulted in a 15 folds increase. In other words, in the presence of DTT, PES triggered a mere increase of 1.5 folds over DTT, indicating that p53 up-regulation was mainly a response to the generation of ROS. Second, we evaluated the production of ROS in p53-null cells stimulated with PES. At times when p53 was up-regulated by PES, HCT116 p53 -/- cells generated significantly lower amounts of ROS than HCT116 cells (Fig. 7B). In sum, we showed ROS up-regulated p53 and p53 promoted ROS generation. Therefore we propose the existence of a positive feed back loop between p53 and ROS in the process of PES-mediated necrosis.

4. Discussion

Here, we describe PES induces cytotoxicity in cell lines of different ontogeny. Cell death by this compound is caspase-independent and presents a prominent cytoplasmic vacuolization. The nuclei of PES-injured cells do not show morphological traits of apoptotic cell death. Moreover, PES promotes an early induction on the intracellular ROS content that, in turn, is a key event for the cytotoxic process. This oxidative stress is responsible of an up-regulation of p53, which participates in PES-driven cell death. Notably, down-regulation or genetic suppression of p53 makes cells more resistant to necrosis induced by PES. Localization of p53 in the chromatin-bound fraction and up-regulation of p21 indicate the involvement of a transcription-dependent p53 program in PES-driven necrosis. Finally, we also present evidence of PES eliciting a positive feedback loop between ROS and p53, which results in the final necrotic outcome.

p53, also known as the “guardian of the genome”, is a pivotal element in the cell response to chemotherapeutic agents. The fact that p53-defective cells remain sensitive to PES-induced cell death is taken as a proof of its irrelevance in the process [2,21]. Nonetheless, up-regulation of p53 in response to PES is reported in multiple cell lines [2,3]. There exists only one exception in which PES triggers p53-independent apoptosis, without p53 up-regulation [21]. Under these premises, we interrogated the involvement of p53 in genetically modified experimental paradigms: HCT116 and their isogenic HCT116 p53-/-, HCT116 p53-/- cells overexpressing a functional p53, and, finally, HCT116 and SH-SY5Y cells with diminished levels of p53. Regardless of the genetically modified paradigm, p53 exerted a positive role, increasing PES-triggered necrosis. Moreover, we have provided evidences of p53 transcriptional involvement since p53

remains in the appropriate nuclear compartment for transcription modulation and content of p21 is increased.

Blockade of RNA polymerase II-mediated transcription induces p53 accumulation in mitochondria, being the critical factor for eliciting p53-dependent, but transcription-independent, apoptosis [33]. On the contrary, PES is a well-known inhibitor of p53 translocation to mitochondria [1] with no reported effects on transcription. Applying the former reasoning, PES-driven global increase of p53, having its movement to the mitochondria impeded, could act as a permissive event for p53 transcription-dependent necrosis to occur. Despite our findings, high concentrations of PES are cytotoxic in HCT116 p53-/- cells. Our explanation to this phenomenon is the loss of drug specificity at the highest concentrations employed. Our data also evidence that PES triggers cell death in p53-null cells, such as HL-60. In this regard, when high concentrations of PES are used, we cannot rule out the involvement of other members of the p53 family of transcription factors, such as p63 or p73, which all share amino acid sequence identity in the DNA-binding domain, and thus could present redundant functions in the regulation of gene expression [34].

The critical role of ROS in the regulation of necrotic pathways [35,36], prompted us to characterize them in our paradigms. Oxidative stress occurs as a consequence of the imbalance between the rate of ROS production and neutralization by specific detoxifying proteins, frequently leading cells to death either by apoptosis or necrosis. We found an accumulation of ROS at times as early as 30 min after PES treatment. Moreover, thiolic antioxidants conferred the highest protection facing PES when compared to the other compounds tested (Fig. 3A). To our knowledge, only one report

exists about ROS involvement in the lethal mode of action of PES [22]. However, the authors show that PES triggers apoptosis rather than necrosis. Two main issues need to be taken into account in their work: the delayed kinetics of ROS accumulation, starting at 4 h of treatment, and the non-tumor origin of their cellular model, which is based on rainbow trout, gill-derived, cells. In addition we report a pharmacological cooperation between PES and BSO that translates into an increased ROS content and a greater cytotoxicity. This cooperation reinforces our conclusion about PES-mediated ROS generation but, in addition, it raises strategic implications for cancer therapy. In our laboratory, we have observed BSO to be minimally toxic for cells unless subjected to other simultaneous stresses. This is consistent with BSO being well tolerated by humans in clinical assays [37,38]. The association of BSO and anticancer drugs in not new, it has been described, for example, with retinoids in neuroblastoma [39], melphalan or cisplatin in ovarian cancer [40,41], vitamin D in breast cancer [42], or azathioprine in colon and hepatic carcinoma [43]. We have no knowledge about PES toxicity in humans. However, BSO combined to PES will probably allow the reduction of PES doses, not decreasing its efficacy and minimizing its nonspecific effects.

Multiple lines of evidence exist on the mutual regulation of p53 and ROS. For instance, DNA damage by ROS triggers an alarm response with p53 as the central player. Moreover, ROS activate phosphorylation cascades trough p38α MAPK and ERK ending up in p53 stabilization [44]. Finally, oxidation of cysteine residues in p53 modifies its DNA binding activity and the transcription of specific genes [45]. Our data evidenced ROS inhibition attenuates p53 increase in response to PES, thus positioning ROS upstream of p53 up-regulation. On the other hand, p53 can promote ROS generation by

transcriptionally inducing enzymes, such as quinone oxidoreductase or proline oxidase, or pro-oxidant genes, such as *BAX*, *PUMA* and $p66^{Shc}$ [45]. Similarly, p53-mediated suppression of antioxidant genes such as manganese superoxide dismutase (*MnSOD*), could finally impinge on the ROS content [45]. Though p53 is known to respond to ROS by inducing either anti-oxidant or pro-oxidant genes, it has been suggested that the severity of the stimulus could be critical in making this decision [46]. In support of the pro-oxidant role of p53, we found that HCT116 p53-/- cells generate a limited amount of ROS when compared to HCT116 (Fig. 7B).

Our results using multiple cell lines are consistent with previous data reporting PES elicits a caspase-independent cell death characterized by a prominent cytoplasmic vacuolization [2]. The same authors report a null effect of up-regulating the anti-apoptotic BCL-X_L protein on PES-induced cell demise. In the same line, we have found that MEF *Bax-/-Bak-/-* cells remain fully sensitive to PES-triggered cell death. Since these cells are fully resistant to apoptosis through the intrinsic pathway [15], these data prove that death pathways engaged by PES are clearly unrelated to apoptosis. Consistently, in primary effusion lymphoma PES triggers a caspase-independent cell death mediated by lysosomal permeabilization [19]. Nonetheless, in other cellular models, apoptosis seems to be the main type of cell death caused by PES [20–22]. To complete the picture, a simultaneous mixture of both caspase-dependent and independent cell death was found in pancreatic cell lines treated with PES [23]. These data, which seem to be contradictory, can be explained by differences in the cell death behavior, inherent to each cellular model. Alternatively, taking into account our results, another plausible explanation would be the different cellular ability to buffer PES-driven

oxidative stress. Indeed, it is broadly accepted that ROS have the capability to modulate apoptosis. For instance, low concentrations of H_2O_2 trigger caspase-dependent apoptosis while higher amounts elicit necrosis and impair caspase activation [47]. In this sense, it is known that direct oxidation of the cysteine from the catalytic center of caspases is able to inhibit these proteases [47]. Along the same line, our results prove first, that PES is unable to promote the activation of caspases in multiple cell lines (Fig. 2 A, B and C) and second, that the pan-caspase inhibitor Q-VD-OPh is unable to protect cells from PES-driven necrosis (Fig. 3A).

Pioneer studies cataloged cell death processes into three main morphological categories: apoptosis, autophagic cell death and necrosis. Through time, the need of a more precise definition has become evident and the evaluation of new biochemical parameters has implemented the original classification [48]. Similarly, pharmacological strategies have been set up to distinguish between these processes of cell death. 3-MA and Spautin-1 are compounds known for its activity suppressing autophagy [49–51]. Our data showed neither 3-MA nor Spautin-1 were able to block cell death in response to PES. The absence of protection suggests the induction of autophagy is not involved in the mechanism of death by PES. Additionally, it is known that PES impairs the autophagy-lysosome systems, resulting in a accumulation of autophagic vacuoles and generation of proteotoxic stress [2,19]. Furthermore, combination of PES with 3-MA or Spautin-1 enhances cytotoxicity in SH-SY5Y cells, thus suggesting autophagy could be playing a protective role, instead. MEFs *Atg5-/-* are unable to perform the classical autophagy pathway [52] and thus, they are a valuable tool to study the involvement of autophagy under different settings. Experiments from our laboratory have revealed that

MEFs *Atg5-/-* display a greater susceptibility to PES-driven death (data not shown). We believe these results are consistent with the role of autophagy attenuating proteotoxicity [53] and thus, diminishing the proteotoxic stress inflicted by PES.

Necrosis is morphologically characterized by rounding of the cell, a gain in cell volume (also known as oncosis), organelle swelling, lack of internucleosomal DNA fragmentation, and plasma membrane rupture [54]. Despite its early association to accidental forms of cell death, new data link it to regulated forms of cell demise, otherwise known as “programmed necrosis”. In this sense, necroptosis is currently the best characterized form of programmed necrosis [55]. In our experiments, the absence of protective effects of the combination of Necrostatin-1 and PES, indicates PES triggers a non-necroptotic necrosis. While the physiological relevance of alternative forms of cell death remains under study, there is no doubt about the spontaneous appearance of mechanisms to elude them. These mechanisms are clearly linked to chemoresistance in cancer. For instance, overexpression of PDIA6, a protein disulfide isomerase, is one of the mechanisms accountable for the increased chemoresistance of lung adenocarcinoma to cisplatin-induced necroptosis [56]. Similarly, ROS-induced miR-21 promotes apoptotic resistance of vascular smooth muscle cells to oxidative stress [57]. Infectious myocarditis presents both forms of cell death: apoptosis and necrosis. Forced expression of miR-21 reduces apoptotic myocarditis through the down-regulation of programmed cell death 4 (PDCD4) messenger [58]. Nevertheless, the overexpression of the same microRNA has no impact reducing necrotic-type myocarditis [58]. In conclusion, we believe that inducers of non-canonical forms of programmed necrosis harbor a great potential for new-line pharmacological therapies.

REFERENCES

[1] Strom E, Sathe S, Komarov PG, Chernova OB, Pavlovska I, Shyshynova I, et al. Small-molecule inhibitor of p53 binding to mitochondria protects mice from gamma radiation. Nat Chem Biol 2006;2:474–9.

[2] Leu J, Pimkina J, Frank A, Murphy M, George D. A small molecule inhibitor of inducible heat shock protein 70. Mol Cell 2009;36:15–27.

[3] Leu JI-J, Pimkina J, Pandey P, Murphy ME, George DL. HSP70 inhibition by the small-molecule 2-phenylethynesulfonamide impairs protein clearance pathways in tumor cells. Mol Cancer Res 2011;9:936–47.

[4] Vousden KH, Prives C. Blinded by the Light: The Growing Complexity of p53. Cell 2009;137:413–31.

[5] Hollstein M, Sidransky D, Vogelstein B, Harris CC. p53 mutations in human cancers. Science 1991;253:49–53.

[6] Hollstein M, Shomer B, Greenblatt M, Soussi T, Hovig E, Montesano R, et al. Somatic point mutations in the p53 gene of human tumors and cell lines: updated compilation. Nucleic Acids Res 1996;24:141–6.

[7] Liu B, Chen Y, St Clair DK. ROS and p53: a versatile partnership. Free Radic Biol Med 2008;44:1529–35.

[8] Bieging KT, Attardi LD. Deconstructing p53 transcriptional networks in tumor suppression. Trends Cell Biol 2012;22:97–106.

[9] Zong WX, Thompson CB. Necrotic death as a cell fate. Genes Dev 2006;20:1–15.

[10] Moubarak RS, Yuste VJ, Artus C, Bouharrour A, Greer PA, Menissier-de Murcia J, et al. Sequential activation of poly(ADP-ribose) polymerase 1, calpains, and Bax is essential in apoptosis-inducing factor-mediated programmed necrosis. Mol Cell Biol 2007;27:4844–62.

[11] Ribas J, Yuste VJ, Garrofe-Ochoa X, Meijer L, Esquerda JE, Boix J. 7-Bromoindirubin-3'-oxime uncovers a serine protease-mediated paradigm of necrotic cell death. Biochem Pharmacol 2008;76:39–52.

[12] Vanden Berghe T, Linkermann A, Jouan-Lanhouet S, Walczak H, Vandenabeele P. Regulated necrosis: the expanding network of non-apoptotic cell death pathways. Nat Rev Mol Cell Biol 2014;15:135–47.

[13] Bunz F, Dutriaux A, Lengauer C, Waldman T, Zhou S, Brown JP, et al. Requirement for p53 and p21 to sustain G2 arrest after DNA damage. Science 1998;282:1497–501.

[14] Wei MC, Zong WX, Cheng EH, Lindsten T, Panoutsakopoulou V, Ross AJ, et al. Proapoptotic BAX and BAK: a requisite gateway to mitochondrial dysfunction and death. Science (80-) 2001;292:727–30.

[15] Lindsten T, Ross A, King A, Zong W. The combined functions of proapoptotic Bcl-2 family members bak and bax are essential for normal development of multiple tissues. Mol Cell 2000;6:1389–99.

[16] Ribas J, Gomez-Arbones X, Boix J. Caspase 8/10 are not mediating apoptosis in neuroblastoma cells treated with CDK inhibitory drugs. Eur J Pharmacol 2005;524:49–52.

[17] Baker SJ, Markowitz S, Fearon ER, Willson JK, Vogelstein B. Suppression of human colorectal carcinoma cell growth by wild-type p53. Science (80-) 1990;249:912–5.

[18] Iglesias-Guimarais V, Gil-Guiñon E, Gabernet G, García-Belinchón M, Sánchez-Osuna M, Casanelles E, et al. Apoptotic DNA degradation into oligonucleosomal fragments, but not apoptotic nuclear morphology, relies on a cytosolic pool of DFF40/CAD endonuclease. J Biol Chem 2012;287:7766–79.

[19] Granato M, Lacconi V, Peddis M, Lotti L V, Renzo LD, Gonnella R, et al. HSP70 inhibition by 2-phenylethynesulfonamide induces lysosomal cathepsin D release and immunogenic cell death in primary effusion lymphoma. Cell Death Dis 2013;4:305–13.

[20] Balaburski GM, Leu JI-J, Beeharry N, Hayik S, Andrake MD, Zhang G, et al. A modified HSP70 inhibitor shows broad activity as an anticancer agent. Mol Cancer Res 2013;11:219–29.

[21] Steele AJ, Prentice AG, Hoffbrand A V, Yogashangary BC, Hart SM, Lowdell MW, et al. 2-Phenylacetylenesulfonamide (PAS) induces p53-independent apoptotic killing of B-chronic lymphocytic leukemia (CLL) cells. Blood 2009;114:1217–25.

[22] Zeng F, Tee C, Liu M, Sherry JP, Dixon B, Duncker BP, et al. The p53/HSP70 inhibitor, 2-phenylethynesulfonamide, causes oxidative stress, unfolded protein response and apoptosis in rainbow trout cells. Aquat Toxicol 2014;146:45–51.

[23] Monma H, Harashima N, Inao T, Okano S, Tajima Y, Harada M. The HSP70 and autophagy inhibitor pifithrin-μ enhances the antitumor effects of TRAIL on human pancreatic cancer. Mol Cancer Ther 2013;12:341–51.

[24] Griffith OW, Meister A. Potent and specific inhibition of glutathione synthesis by buthionine sulfoximine (S-n-butyl homocysteine sulfoximine). J Biol Chem 1979;254:7558–60.

[25] Armstrong JS, Steinauer KK, Hornung B, Irish JM, Lecane P, Birrell GW, et al. Role of glutathione depletion and reactive oxygen species generation in apoptotic signaling in a human B lymphoma cell line. Cell Death Differ 2002;9:252–63.

[26] Dorr R, Liddil J, Soble M. Cytotoxic effects of glutathione synthesis inhibition by L-buthionine-(SR)-sulfoximine on human and murine tumor cells. Invest New Drugs 1986;4.

[27] Montero J, Dutta C, van Bodegom D, Weinstock D, Letai A. p53 regulates a non-apoptotic death induced by ROS. Cell Death Differ 2013;20:1465–74.

[28] Tu HC, Ren D, Wang GX, Chen DY, Westergard TD, Kim H, et al. The p53-cathepsin axis cooperates with ROS to activate programmed necrotic death upon DNA damage. Proc Natl Acad Sci U S A 2009;106:1093–8.

[29] Vaseva A, Marchenko N, Ji K. p53 opens the mitochondrial permeability transition pore to trigger necrosis. Cell 2012;149:1536–48.

[30] Beckerman R, Prives C. Transcriptional regulation by p53. Cold Spring Harb Perspect Biol 2010;2:a000935.

[31] Dulic V, Kaufmann WK, Wilson SJ, Tlsty TD, Lees E, Harper JW, et al. p53-dependent inhibition of cyclin-dependent kinase activities in human fibroblasts during radiation-induced G1 arrest. Cell 1994;76:1013–23.

[32] el-Deiry WS, Tokino T, Velculescu VE, Levy DB, Parsons R, Trent JM, et al. WAF1, a potential mediator of p53 tumor suppression. Cell 1993;75:817–25.

[33] Arima Y, Nitta M, Kuninaka S, Zhang D, Fujiwara T, Taya Y, et al. Transcriptional blockade induces p53-dependent apoptosis associated with translocation of p53 to mitochondria. J Biol Chem 2005;280:19166–76.

[34] Levrero M, De Laurenzi V, Costanzo A, Gong J, Wang JY, Melino G. The p53/p63/p73 family of transcription factors: overlapping and distinct functions. J Cell Sci 2000;113:1661–70.

[35] Maryanovich M, Gross A. A ROS rheostat for cell fate regulation. Trends Cell Biol 2013;23:129–34.

[36] Scherz-Shouval R, Elazar Z. Regulation of autophagy by ROS: physiology and pathology. Trends Biochem Sci 2011;36:30–8.

[37] Anderson CP, Seeger RC, Satake N, Monforte-Munoz HL, Keshelava N, Bailey HH, et al. Buthionine sulfoximine and myeloablative concentrations of melphalan overcome resistance in a melphalan-resistant neuroblastoma cell line. J Pediatr Hematol Oncol 2001;23:500–5.

[38] Bailey HH, Mulcahy RT, Tutsch KD, Arzoomanian RZ, Alberti D, Tombes MB, et al. Phase I clinical trial of intravenous L-buthionine sulfoximine and melphalan: an attempt at modulation of glutathione. J Clin Oncol 1994;12:194–205.

[39] Cuperus R, van Kuilenburg ABP, Leen R, Bras J, Caron HN, Tytgat GAM. Promising effects of the 4HPR-BSO combination in neuroblastoma monolayers and spheroids. Free Radic Biol Med 2011;51:1213–20.

[40] Ozols RF, Louie KG, Plowman J, Behrens BC, Fine RL, Dykes D, et al. Enhanced melphalan cytotoxicity in human ovarian cancer in vitro and in tumor-bearing nude mice by buthionine sulfoximine depletion of glutathione. Biochem Pharmacol 1987;36:147–53.

[41] Chen G, Zeller WJ. Augmentation of cisplatin (DDP) cytotoxicity in vivo by DL-buthionine sulfoximine (BSO) in DDP-sensitive and-resistant rat ovarian tumors and its relation to DNA interstrand cross links. Anticancer Res n.d.;11:2231–7.

[42] Bohl LP, Liaudat AC, Picotto G, Marchionatti AM, Narvaez CJ, Welsh J, et al. Buthionine sulfoximine and 1,25-dihydroxyvitamin D induce apoptosis in breast cancer cells via induction of reactive oxygen species. Cancer Invest 2012;30:560–70.

[43] Hernández-Breijo B, Monserrat J, Ramírez-Rubio S, Cuevas EP, Vara D, Díaz-Laviada I, et al. Preclinical evaluation of azathioprine plus buthionine sulfoximine in the treatment of human hepatocarcinoma and colon carcinoma. World J Gastroenterol 2011;17:3899–911.

[44] Bragado P, Armesilla A, Silva A, Porras A. Apoptosis by cisplatin requires p53 mediated p38alpha MAPK activation through ROS generation. Apoptosis 2007;12:1733–42.

[45] Liu B, Chen Y, St Clair DK. ROS and p53: a versatile partnership. Free Radic Biol Med 2008;44:1529–35.

[46] Sablina AA, Budanov A V, Ilyinskaya G V, Agapova LS, Kravchenko JE, Chumakov PM. The antioxidant function of the p53 tumor suppressor. Nat Med 2005;11:1306–13.

[47] Hampton MB, Fadeel B, Orrenius S. Redox regulation of the caspases during apoptosis. Ann N Y Acad Sci 1998;854:328–35.

[48] Galluzzi L, Vitale I, Abrams JM, Alnemri ES, Baehrecke EH, Blagosklonny M V, et al. Molecular definitions of cell death subroutines: recommendations of the Nomenclature Committee on Cell Death 2012. Cell Death Differ 2012;19:107–20.

[49] Seglen PO, Gordon PB. 3-Methyladenine: specific inhibitor of autophagic/lysosomal protein degradation in isolated rat hepatocytes. Proc Natl Acad Sci U S A 1982;79:1889–92.

[50] Tsujimoto Y, Shimizu S. Another way to die: autophagic programmed cell death. Cell Death Differ 2005;12 Suppl 2:1528–34.

[51] Liu J, Xia H, Kim M, Xu L, Li Y, Zhang L, et al. Beclin1 controls the levels of p53 by regulating the deubiquitination activity of USP10 and USP13. Cell 2011;147:223–34.

[52] Kuma A, Hatano M, Matsui M, Yamamoto A, Nakaya H, Yoshimori T, et al. The role of autophagy during the early neonatal starvation period. Nature 2004;432:1032–6.

[53] Rubinsztein DC, Mariño G, Kroemer G. Autophagy and aging. Cell 2011;146:682–95.

[54] Laster SM, Wood JG, Gooding LR. Tumor necrosis factor can induce both apoptic and necrotic forms of cell lysis. J Immunol 1988;141:2629–34.

[55] Vandenabeele P, Galluzzi L, Vanden Berghe T, Kroemer G. Molecular mechanisms of necroptosis: an ordered cellular explosion. Nat Rev Mol Cell Biol 2010;11:700–14.

[56] Tufo G, Jones AWE, Wang Z, Hamelin J, Tajeddine N, Esposti DD, et al. The protein disulfide isomerases PDIA4 and PDIA6 mediate resistance to cisplatin-induced cell death in lung adenocarcinoma. Cell Death Differ 2014;21:685–95.

[57] Lin Y, Liu X, Cheng Y, Yang J, Huo Y, Zhang C. Involvement of MicroRNAs in hydrogen peroxide-mediated gene regulation and cellular injury response in vascular smooth muscle cells. J Biol Chem 2009;284:7903–13.

[58] He J, Yue Y, Dong C, Xiong S. MiR-21 confers resistance against CVB3-induced myocarditis by inhibiting PDCD4-mediated apoptosis. Clin Invest Med 2013;36:E103–11.

Acknowledgments–We thank Dr. Mario Encinas, Dr. Xavier Dolcet and Dr. Núria Eritja for providing the FSV and FSV shRNA p53 vectors. We are grateful to Dr. Gabriel Gil for supplying the pCMV-Neo-Bam and pCMV-Neo-Bam p53 plasmids.

FOOTNOTES

* This work was supported by Spanish Government, MINECO (Ministerio de Economía y Competitividad), project SAF2011-29730. Paolo Mattiolo was supported by a FI fellowship -AH9815758- from AGAUR (Generalitat de Catalunya) .

[1] Contributed equally to the work

[2] Senior co-authors

FIGURE LEGENDS

FIGURE 1. PES-driven cell death is concentration and time dependent. A. The cell lines indicated in the graph were treated for 24 h with increasing concentrations of PES. Cell viability was calculated by the MTS reduction assay. B. SH-SY5Y and C, HCT116 WT cells were exposed to the indicated concentrations of PES. Cell death by PI staining was quantified over time. Each value in the graphical representation is the average ± S.D. of at least 3 independent experiments with 3 independent measurements per experiment.

FIGURE 2. PES triggers caspase-independent non-apoptotic cell death. A. SH-SY5Y cells were challenged with 12.5 μM PES or STS 250 nM and the time course of caspase activation (DEVDase activity) was determined. Activity is measured in arbitrary fluorescence units (a.f.u). Each point is the average ± S.D. of 6 independent measurements. The plotted profile is representative of 3 independent experiments. ***P<0.001 (Student's t-test referred to time 0). B. HCT116 cells were treated with 25 μM PES or 250 nM STS and processed as in A. C. U87MG, HeLa, 293HEK and HL-60 were subjected for 12 h to 20, 25, 50 or 15 μM PES respectively. In parallel, cells were exposed to vehicle (V) or STS 250 nM for 12 h. Caspase activation (DEVDase activity) was quantified as above. D. MEF defective in BAX and BAK proteins and their WT controls were treated for 24 h with 30 μM PES or, alternatively, with 1 μM STS. Cell viability was measured by the MTS reduction assay. Bar value is the mean ± S.D. of at least 3 independent determinations in 3 independent experiments.

FIGURE 3. PES triggers a non-necroptotic, necrotic type of cell death. A. After a preincubation of 3 h with 10 μM QVD-OPh (QVD), 25 μM Necrostatin-1 (Nec), 10 mM 3-MA (3-MA) or 10 μM Spautin-1 (Spautin), PES was added for 12 h at a concentration of 25 μM for HCT116 and 12.5 μM for SH-SY5Y cells. A control of vehicle-treated cells was included (C). Cell survival was quantified by Alamar blue. When a combined treatment was performed (PES + inhibitor), Alamar blue values were referred to the ones of the cells treated with the inhibitor alone. Bar value is the mean± S.D. of at least 3 independent experiments with three independent measurements per experiment. **P< 0.005 (Student's t-test referred to PES-treated control). B. Transmission electron microscopy of HCT116 in untreated conditions. C. HCT116 cells treated for 48h with 25 μM PES, displaying an early necrotic phenotype. D. HCT116 treated as in C, showing a more advanced necrotic phenotype. Arrows indicate areas of discontinued plasmatic membrane. E. Control SH-SY5Y cells untreated. F. SH-SY5Y cells treated with 12.5 μM PES for 12h. Arrowhead indicates the multilamellar autophagosome structure shown at higher resolution in the inset. Nu: Nuclear chromatin. G: Golgi apparatus. m: mitochondria. Black asterisks: Vacuoles. White asterisks: Dilated mitochondria with disrupted cristae.

FIGURE 4. ROS are pivotal elements in necrosis by PES. A. HCT116 cells were treated with 25 μM PES or DMSO (Vehicle) for the times indicated in the x-axis. Quantification of ROS was performed as described in the methods section and expressed as arbitrary fluorescence units (a.f.u) generated by DCF. B. SH-SY5Y cells were pre-incubated for 1 h with 1.25 mM NAC or 500 μM DTT before adding 12.5 μM PES or DMSO (Vehicle) for

an additional 24 h period. Cell death was measured by flow cytometry and the count of PI stained cells. C. HCT116 cells were treated with 25 μM PES for 48 h and analyzed as reported for SH-SY5Y in B. ***P<0.001 (Student's t-test referred to PES-treated control). D. HCT116 and SH-SY5Y cells were either pre-incubated with BSO or left untreated. After a 3 h pre-incubation, PES was added at 6.25 μM for an extra 8 h period. ROS fluorescent signal was referred to the one of the DMSO (Vehicle) treated cells. ***P<0.001 (Student's t-test referred to PES-treated control). E. Cell lines indicated in the x-axis were pre-incubated for 3 h with 50 μM BSO or left untreated. PES was then added at the concentrations reported in the x-axis. Cell survival was determined by the Alamar blue procedure. Bar value is the average ± S.D. of at least 3 independent experiments with 3 independent measurements. ***P<0.001 (Student's t-test referred to PES-treated control).

FIGURE 5. p53 participates in PES-driven necrosis. A. HCT116 WT and HCT116 p53-/- cells were challenged with the indicated concentrations of PES for a period of 24 h. Cell survival was assessed by MTS reduction. Plots represent the average ± S.D. of at least 3 independent experiments with 3 independent determinations. B. HCT116 and HCT116 p53-/- were treated for 48 h with 25 μM PES. Cell death was determined by flow cytometry count of PI stained cells. Bar value equals mean ± S.D. of at least 3 independent experiments with 3 independent measurements. C. HCT116 p53-/- cells transfected with a plasmid carrying a functional p53 (p53) or empty (Vector) were subjected to PES treatment. Cell survival by MTS reduction was evaluated after 24 h.

Results are the average ± S.D. of at least 3 independent experiments with 3 independent determinations. **P< 0.005 ; ***P<0.001 (Student's t-test).

FIGURE 6. p53 is predominantly located at the chromatin-bound subfractions in response to PES. A. SH-SY5Y cells were treated for 6 h with PES 12.5 μM (P), Staurosporine 1 μM (STS) or left untreated (C). Cells were next subjected to subfractionated extractions as reported in the text. Cytosolic (Cyt), nucleoplasmic (N1) and chromatin-enriched (N2) extracts were obtained. These extracts were analyzed by Western-blot with p53, LDH and PTBP1 antibodies as stated in the figure. NB refers to the membrane stained with naphtol blue to assess an even loading of protein per fraction. Next to the image the quantitation of p53 content in N1 and N2 fractions expressed as "normalized signal intensity" to the p53 in left untreated extracts (C) and performed as described in the methods section. Results are the average ± S.D. of 2 independent experiments. B. SH-SY5Y cells were treated with PES 12.5 μM for the indicated times. Total extracts were obtained and p53 and p21 content was detected by Western-blot. GAPDH was used to control protein loading. The quantification of p53 and p21 content referred to GAPDH is indicated below each panel. Image is the result of one representative experiment out of two C. HCT116 cells were infected with a virus carrying a shRNA against p53 or an empty one. Cell survival was assessed by MTS and referred to the values of vehicle treated cells. Results are the average ± S.D. of at least 3 independent experiments with 3 independent measurements per experiment. D. SH-SY5Y cells were processed and viability assessed as stated before in C for HCT116. **P< 0.005 ; ***P<0.001 (Student's t-test).

FIGURE 7. ROS and p53 mutually regulates each other in response to PES. A. SH-SY5Y cells were pre-incubated with 500 μM DTT or left untreated. Then exposed to 12.5 μM PES or vehicle for 6 h. Total protein extracts were performed and analyzed by Western-blot with p53 and GAPDH antibodies. GAPDH was used to control the protein load. Below, quantitation of the p53 expressed as "normalized signal intensity" to the p53 in left untreated extracts and performed as described in the methods section. Results are the average ± S.D. of 2 independent experiments. B. HCT116 and HCT116 p53-/- isogenic cells were treated with 25 μM PES for 6 h. Quantification of ROS was referred to a control with DMSO (vehicle). Quantification procedure is described in the methods section and expressed as arbitrary fluorescence units (a.f.u) generated by DCF. *P<0.01; (Student's t-test).

FIGURE 1

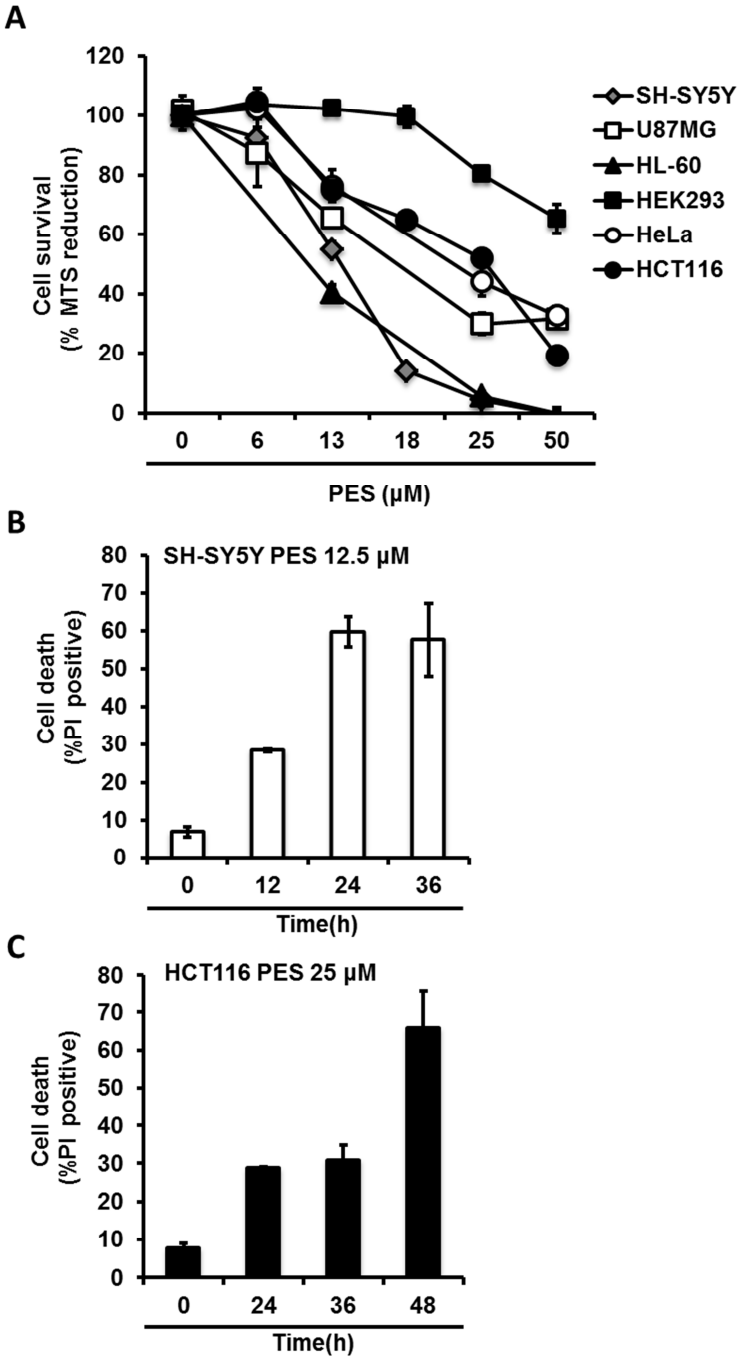
A
120
100
80
60
40
20
0
Cell survival
(% MTS reduction)
0
6
13
18
25
50
PES (μM)
SH-SY5Y
U87MG
HL-60
HEK293
HeLa
HCT116
B
SH-SY5Y PES 12.5 μM
Cell death
(%PI positive)
80
70
60
50
40
30
20
10
0
0
12
24
36
Time(h)
C
HCT116 PES 25 μM
Cell death
(%PI positive)
80
70
60
50
40
30
20
10
0
0
24
36
48
Time(h)

FIGURE 2

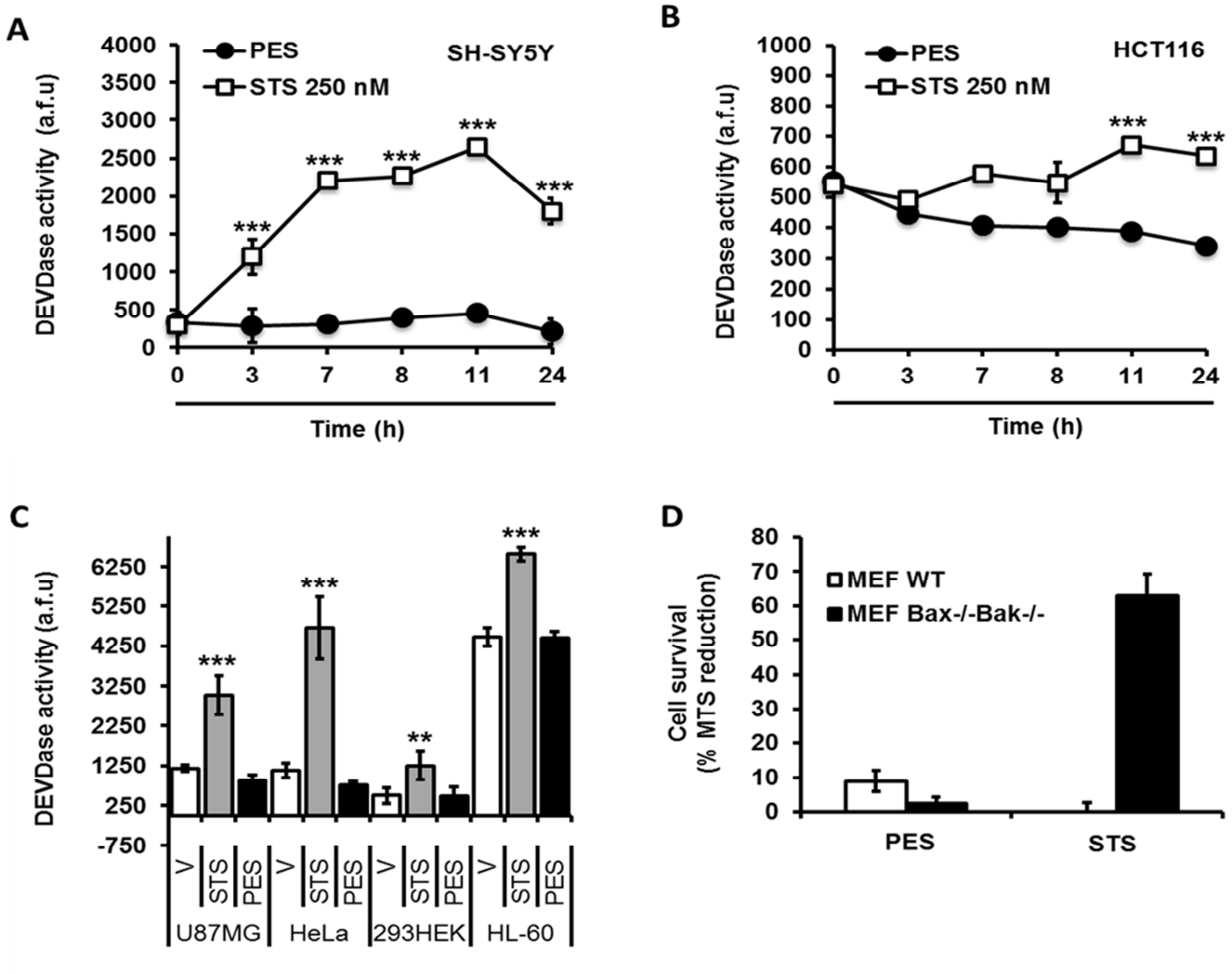
A
PES
STS 250 nM
SH-SY5Y
DEVDase activity (a.f.u)
Time (h)
B
PES
STS 250 nM
HCT116
DEVDase activity (a.f.u)
Time (h)
C
DEVDase activity (a.f.u)
V
STS
PES
U87MG
HeLa
293HEK
HL-60
D
MEF WT
MEF Bax-/-Bak-/-
Cell survival
(% MTS reduction)
PES
STS

FIGURE 3

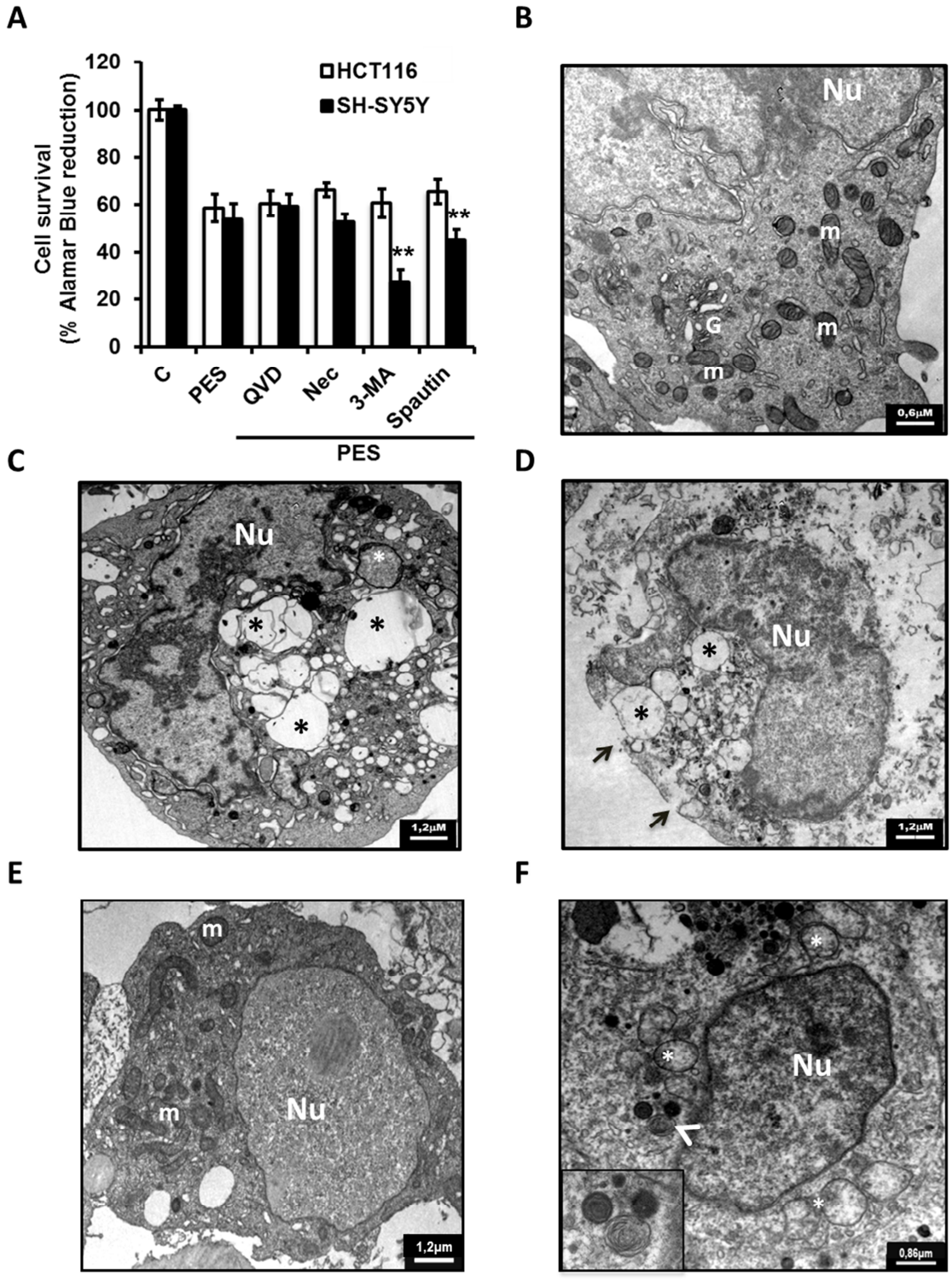
A
B
C
D
E
F
Cell survival
(% Alamar Blue reduction)
120
100
80
60
40
20
0
HCT116
SH-SY5Y
**
**
C
PES
QVD
Nec
3-MA
Spautin
PES
Nu
m
G
m
m
0,6µM
Nu
1,2µM
Nu
1,2µM
m
m
Nu
1,2µm
Nu
0,86µm

FIGURE 4

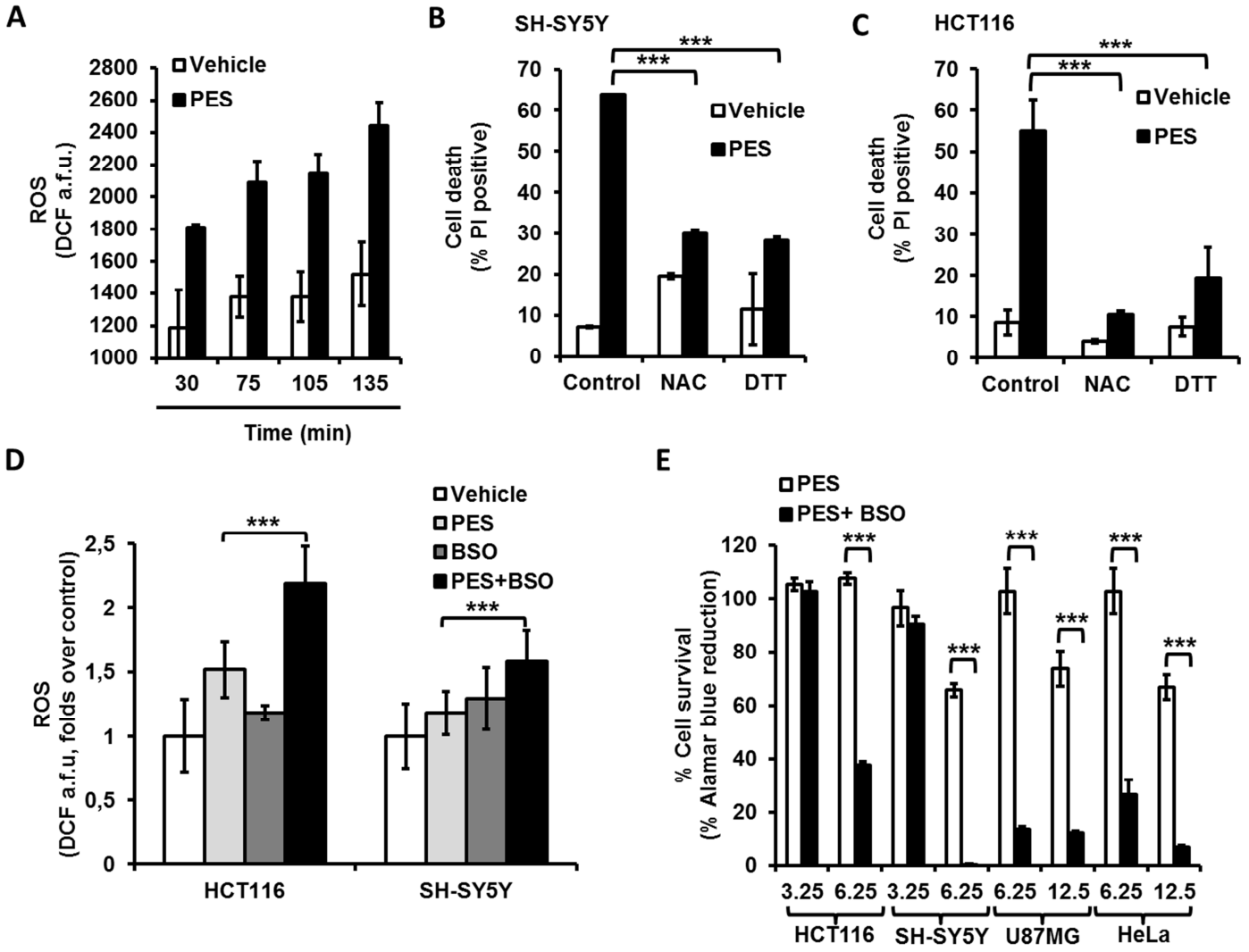
A
ROS
(DCF a.f.u.)
2800
2600
2400
2200
2000
1800
1600
1400
1200
1000
Vehicle
PES
30
75
105
135
Time (min)
B
SH-SY5Y
Cell death
(% PI positive)
70
60
50
40
30
20
10
0
***
***
Vehicle
PES
Control
NAC
DTT
C
HCT116
Cell death
(% PI positive)
70
60
50
40
30
20
10
0
***
***
Vehicle
PES
Control
NAC
DTT
D
ROS
(DCF a.f.u, folds over control)
2,5
2
1,5
1
0,5
0
***
***
Vehicle
PES
BSO
PES+BSO
HCT116
SH-SY5Y
E
PES
PES+ BSO
% Cell survival
(% Alamar blue reduction)
120
100
80
60
40
20
0
***
***
***
***
***
***
3.25
6.25
3.25
6.25
6.25
12.5
6.25
12.5
HCT116
SH-SY5Y
U87MG
HeLa

FIGURE 5

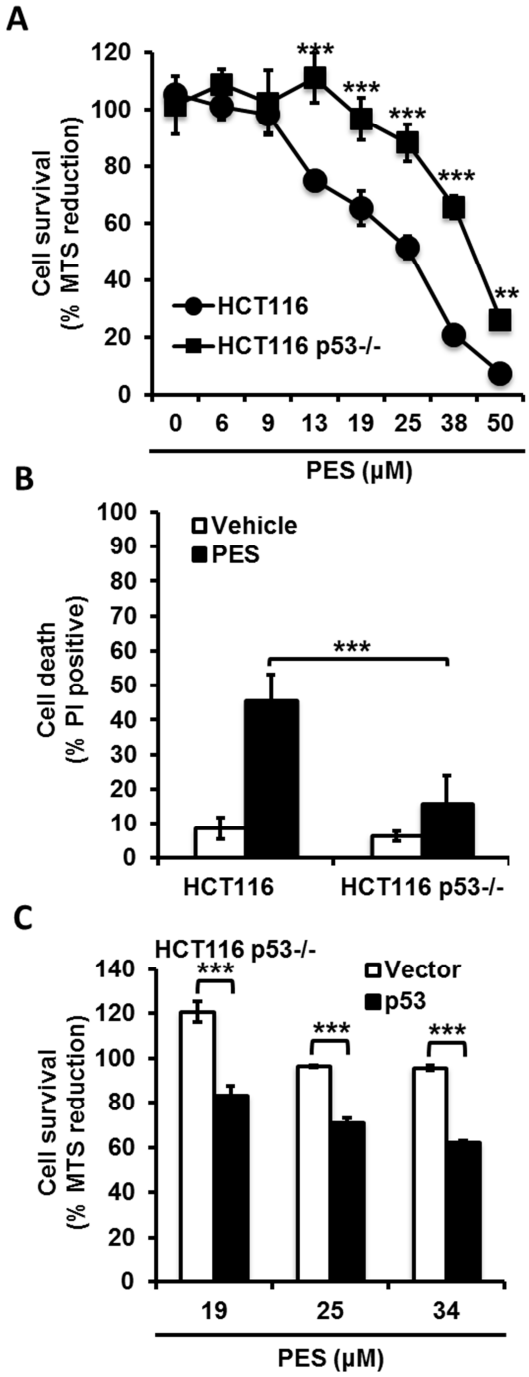
A
Cell survival
(% MTS reduction)
120
100
80
60
40
20
0
***
***
***
***
**
HCT116
HCT116 p53-/-
0 6 9 13 19 25 38 50
PES (μM)
B
Cell death
(% PI positive)
100
90
80
70
60
50
40
30
20
10
0
Vehicle
PES
***
HCT116
HCT116 p53-/-
C
HCT116 p53-/-
Cell survival
(% MTS reduction)
140
120
100
80
60
40
20
0
***
***
***
Vector
p53
19
25
34
PES (μM)

FIGURE 6

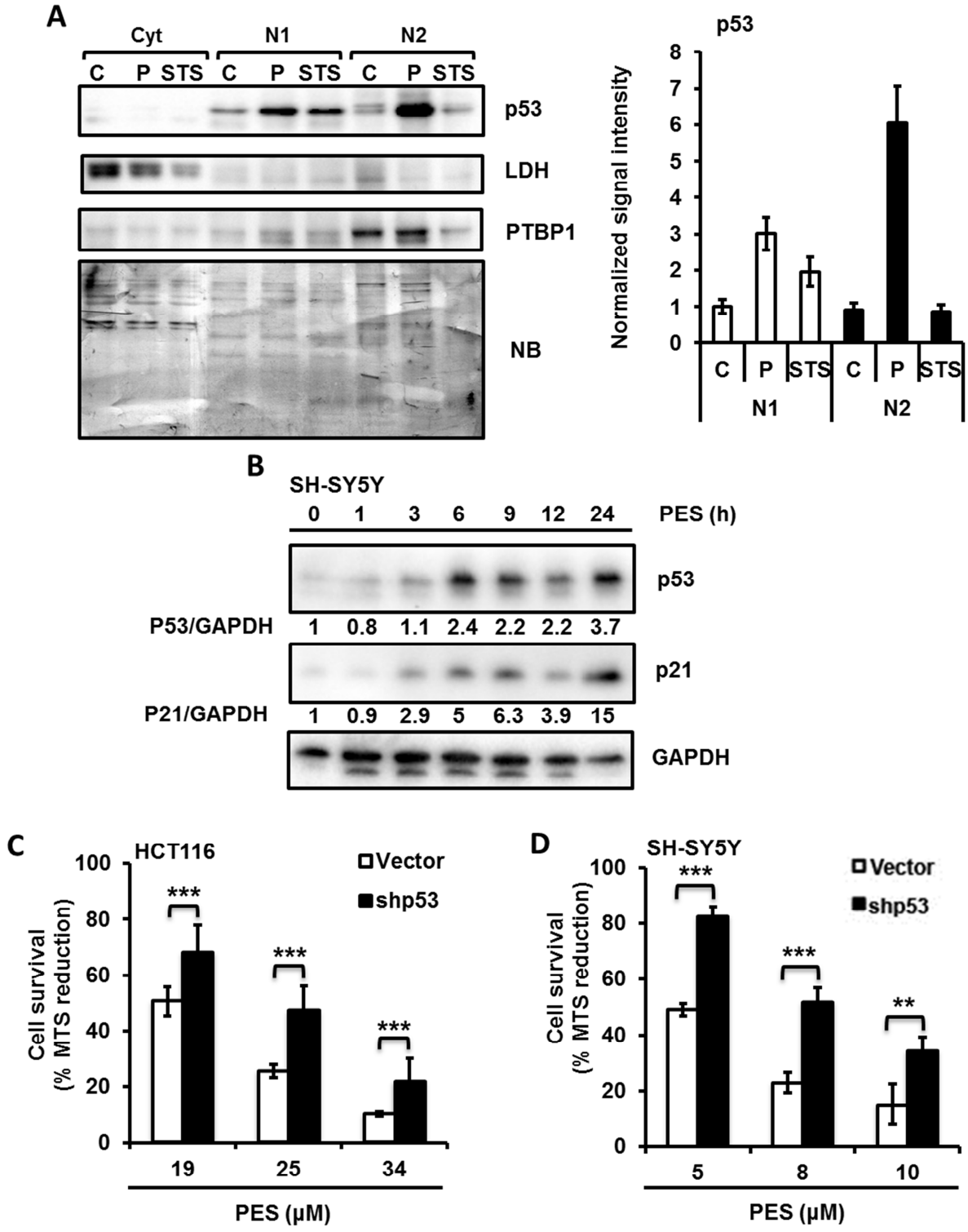
A
Cyt
N1
N2
C P STS C P STS C P STS
p53
LDH
PTBP1
NB
p53
Normalized signal intensity
C P STS C P STS
N1
N2
B
SH-SY5Y
0 1 3 6 9 12 24 PES (h)
p53
P53/GAPDH 1 0.8 1.1 2.4 2.2 2.2 3.7
p21
P21/GAPDH 1 0.9 2.9 5 6.3 3.9 15
GAPDH
C
HCT116
Vector
shp53
Cell survival (% MTS reduction)
19 25 34
PES (μM)
D
SH-SY5Y
Vector
shp53
Cell survival (% MTS reduction)
5 8 10
PES (μM)

FIGURE 7

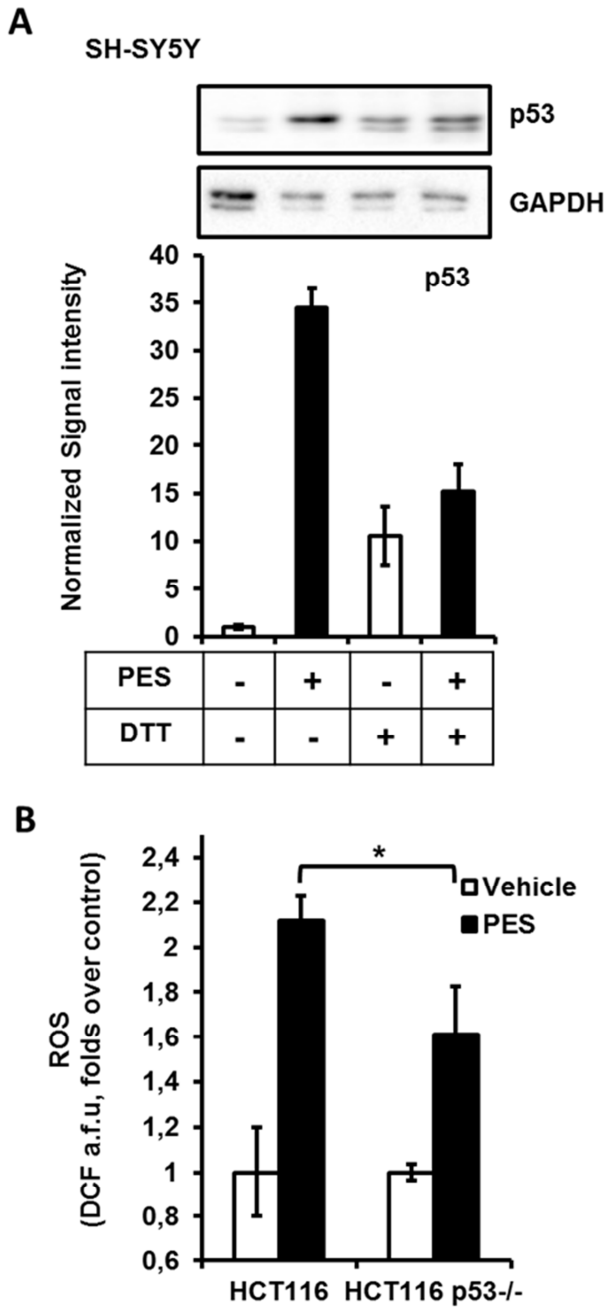
A
SH-SY5Y
p53
GAPDH
p53
Normalized Signal intensity
40
35
30
25
20
15
10
5
0
PES - + - +
DTT - - + +
B
ROS
(DCF a.f.u, folds over control)
2,4
2,2
2
1,8
1,6
1,4
1,2
1
0,8
0,6
*
Vehicle
PES
HCT116
HCT116 p53-/-

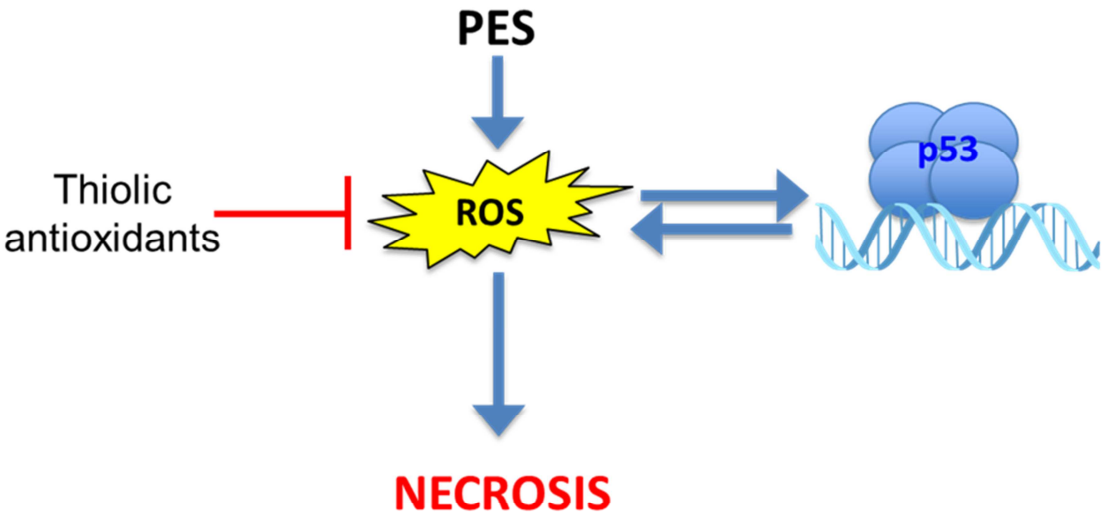

GRAPHICAL ABSTRACT. **2-phenylethynesulfonamide (PES) uncovers a non-necroptotic necrotic cell death regulated by oxidative stress and p53**. Unraveling the cytotoxic mechanisms by PES is of great interest since discovery of its selectivity to kill cancer cells.
Induction of ROS in response to PES up-regulates p53, which in turn increases generation of ROS. These events lead to non-necroptotic necrosis. Avoiding oxidative stress by thiolic antioxidants or suppressing p53 reverts the process.